Diagnostic Analysis Using Textural Features of the Lachrymal Fluid Crystal Images

N.Yu. Ilyasova, A.V. Kupriyanov, A.M. Malapheev, A.G. Khramov
Image Processing Systems Institute of Russian Academy of Sciences
Samara, Russia, akupr@smr.ru

Abstract

The application of the direction field method and the statistical textural analysis for crystallograms classification is proposed. As global features, we took the features the expert uses for the crystallogram-based classification of the eye pathology: unidirectedness of the crystal rays; relative area of domains with clear-cut rays of the crystal; ray density; crystal transparency. As texture features, the instant characteristics of the second order distribution were taken. Experimental studies were conducted on the lachrymal fluid crystallograms.

1. Introduction

Pathological conditions cause multiple changes in the molecular composition of tissue and biological fluid. It is common practice to consider the fluid system as a medium for organism cells. One of techniques to reveal relations between the elements in the system is to transfer the fluid from one phase state into another.

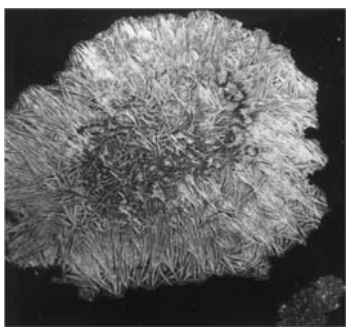

Figure 1. Lachrymal fluid crystallization in the presence of the cuprous chloride

Many authors believe that biological fluids [1] (blood, saliva, urine, and others) are indicative of metabolism impairment caused by the pathology in a human organ. The fluid composition reflects diverse metabolism changes found in the disordered organism. However, examination of the fluid composition commonly involves only the biochemical index. Crystallographic studies (CS) are used as an integrated method that allows one to make implicit conclusions about the matter structure (Figure 1.). Some authors report that the CS of biological fluids can provide information that would allow a more accurate diagnostic of inflammatory, cancer, dystrophic, and allergic diseases. Due to simplicity and high sensitivity, the method has found its way to diagnostics.

2. Formation of crystallogram global diagnostic features

In the recent years, computerized methods for the biomedical image processing have become an important tool of scientific research and enhancement of early diagnostics of various diseases. In clinical practice, crystallogram photographs are analyzed. It is very difficult, and sometimes even impossible, to single out visually the critical pathological signs. In this connection, digital methods for crystallogram image processing are employed. The advantage of computer-aided image analysis is its objectivity and feasibility to quantify the image.

Our studies aim to develop methods for the automated analysis of crystallograms, investigate their diagnostical value, elaborate robust methods for the formalization of medical-diagnostic features, and generate quantitative estimates of pathology probability on the basis of the developed crystallogram classification features. As output the diagnostic system produces an integrated estimate of pathology probability derived from the crystallogram studies, which unites all classification criteria.

According to the crystallographic analysis method used in the clinical practice, the normal eyefluid crystallogram is transparent and comprises thin, mostly unidirectional, clear-cut rays originated from a common crystallization center. Pathological crystals feature a great variety of directions and irregular contours. The pathological crystal is opaque, with numerous ray fractures and bulges. A distinctive feature of pathology is the large density of crystal rays in some areas.

The computerized system for crystallogram analysis is based on the classification of the eye fluid diagnostic features [2]. Thus, by analyzing the crystallograms the ophthalmologist earlier classified as those with and without pathology, we were able to extract the global features the expert uses for the crystallogram-based classification of the eye pathology: unidirectedness of the crystal rays; relative area of domains with clear-cut rays of the crystal; ray density; and crystal transparency.

The quasiperiodic structure is an important feature of the crystallogram images. Because of this, most classification features we discuss are based on the notion of the complex direction field [3] derived from the function of image intensity $I(x, y)$:

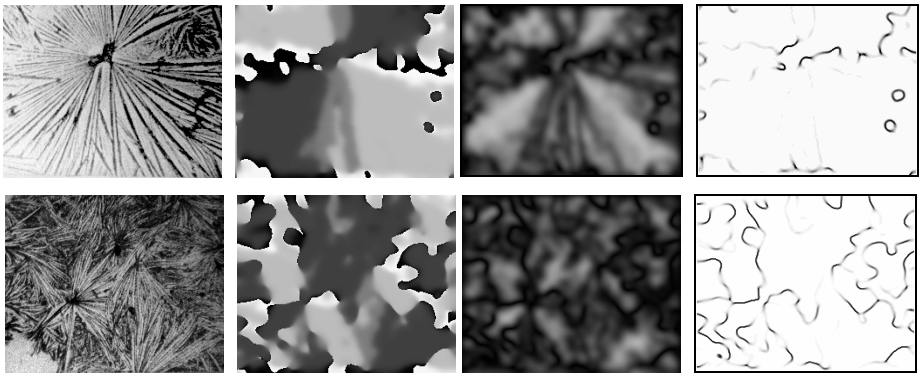

Original image **Filtered direction field** **Weight function** **Contour characteristic**

Figure 2. Characteristic eye fluid crystallogram images and the direction fields in normal (upper row) and pathological condition

$$\dot{\psi}(x,y) = w(x,y)\exp\left(i2\psi(x,y)\right), \quad 0 \le w(x,y) \le 1. \tag{1}$$

$$\operatorname{tg}\psi(x,y) = -\frac{\partial I(x,y)/\partial x}{\partial I(x,y)/\partial y}, \quad 0 \le \psi(x,y) < \pi. \tag{2}$$

The direction field $\psi(x,y)$ represents the tangent angle to the level lines of the intensity function; the weight function $w(x,y)$ has the meaning of the certainty (reliability) in the determination of the direction field at a given point. To discover jumps in the direction field we use the squared modulus of gradient of the complex direction field:

$$\gamma(x,y) = \left|\nabla\dot{\psi}(x,y)\right|^2 = \left|\frac{\partial\dot{\psi}(x,y)}{\partial x}\right|^2 + \left|\frac{\partial\dot{\psi}(x,y)}{\partial y}\right|^2. \tag{3}$$

For the unit weight function, we get

$$\gamma(x,y) = \left(\frac{\partial\sin\psi(x,y)}{\partial x}\right)^2 + \left(\frac{\partial\sin\psi(x,y)}{\partial y}\right)^2 + \left(\frac{\partial\cos\psi(x,y)}{\partial x}\right)^2 + \left(\frac{\partial\cos\psi(x,y)}{\partial y}\right)^2.$$

The value of (3) averaged over the image gives the unidirectedness coefficient K_1.

$$K_1 = \frac{1}{|D|}\iint_D \gamma(x,y)dxdy. \tag{4}$$

The contour characteristic of the direction field of the first pathological crystallogram is depicted in Figure 2. In order to quantify the domains with the pronounced unidirectedness of lines, we use the coefficient of clear-cut lines K2 defined as the ratio of the total area Sp of domains with the greatest values of the weight characteristic of the direction field to the entire image area S :

$$K_2 = S_p / S. \tag{5}$$

Quantitatively, the line density feature in the crystallogram is found to be based on the frequency properties of the image intensity function. As a classification criterion, we take here the mean value of the ray density over the image domain D wherein the weight function takes its greatest value and the value of spectral frequency is certain.

The image intensity function is considered to be locally periodic and admitting the following approximation:

$$I(x,y) = A\sin(\omega_x x + \omega_y y + \varphi) + B, \tag{6}$$

where ωx and ωy are the spatial frequencies to be estimated. The coefficient of the line density K3 is defined as the mean value of the squared spatial frequency of the crystallogram intensity function:

$$K_3 = \frac{1}{(D(}\sum_D \omega^2, \quad \omega^2 = \omega_x^2 + \omega_y^2. \tag{7}$$

The crystallogram transparency is characterized through the probability distribution of the intensity function. The "transparent" crystallogram features a positive shift of the mean value of intensity $\bar{I}$ with respect to the midpoint $I_c = (I_{\max} + I_{\min})/2$ of the intensity range. This criterion can be quantified by the coefficient:

$$K_4 = (\bar{I} - I_c)/\bar{I}. \tag{8}$$

Crystallogram's probability of being pathology-free was used as a criterion for the independent classification by each feature. In particular, the probability is equal to one if the value of the criterion is greater than the threshold of norm, and it is equal to zero if the criterion is smaller than the threshold of pathology. In the intermediate range the dependence is linear. For each feature, the threshold of norm and pathology is chosen from the condition of the minimum classification error under the given criterion. The final estimate of the pathology probability depends on the partial estimates of the pathology probabilities derived from each criterion. Experimental studies [2] have shown that the above-considered features have different weights upon the crystallogram diagnostics.

The weight coefficients for each criterion are taken to be proportional to the classification quality according to the given criterion (the frequency of coincidence of the obtained estimates with a priori ones). The classification results are shown in Table 1. In the table, the column Type indicates the a priori estimate of an image by the ophthalmologist (N - norm, P - pathology); P1 through P4 are the probabilities of norm according to the corresponding classification criteria; R1, R2 are the resulting estimates of the probability of norm obtained via different techniques for combining the classification criteria (R2 is for the optimal combination); C1 and C2 show whether the classification result corresponds to the a priori estimate, provided that threshold is 0.6.

The global diagnostics on a series of samples (150 crystallograms) has made it possible to extract from a variety of crystallograms the normal and pathological groups and quantify the classification features. The error in the pathology recognition in the crystallograms with quasiperiodic structures did not exceed 3-5%. A more detailed processing based on a series of local features will make it possible in the future to go to the differential diagnostics, thus diagnosing separate groups of diseases: tumorous, dystrophic and inflammatory diseases. The objective of the next chapter is studies and formalization of these diagnostics features.

Table 1. The results of classification on the learning sample

Image	Field of directions	Type	P1	P2	P3	P4	R1	C1	R2	C2
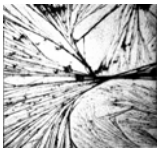		N	0.634	0.4	0.964	1	0.72	+	0.736	+
		N	1	1	0.44	0.294	0.72	+	0.783	+
	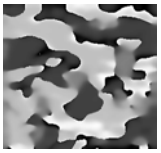	P	0	0	1	0	0.15	+	0.319	+
		N	0.863	1	0.476	0.824	0.83	+	0.751	+
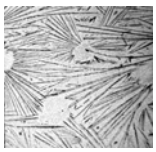		P	0.614	0.525	0.456	1	0.67	-	0.576	+

3. Formation of crystallogram local textural diagnostic features

The image texture is analyzed to provide a series of features for the classification of the eye fluid crystallograms according to the familiar types of pathologies. The textural features were formed on the basis of human visual perception. The aim was to extract the information, which a human interpreter associates connects with the texture.

The different images present a particular texture for each class of the crystallograms that is a global representation of the crystal. A clinical expert extracted seven main classes according to the severity of pathology. The first two classes form a norm group. The last five classes form a pathology group (see Figure 3). The crystallograms available for this study came from 70 patients with different types of pathologies. The texture analysis was carried out on the images of eyefluid crystallograms using the second-order statistics of the gray levels. The gray-level-cooccurrence features [4] have proven to be very successful in the extraction of textural information.

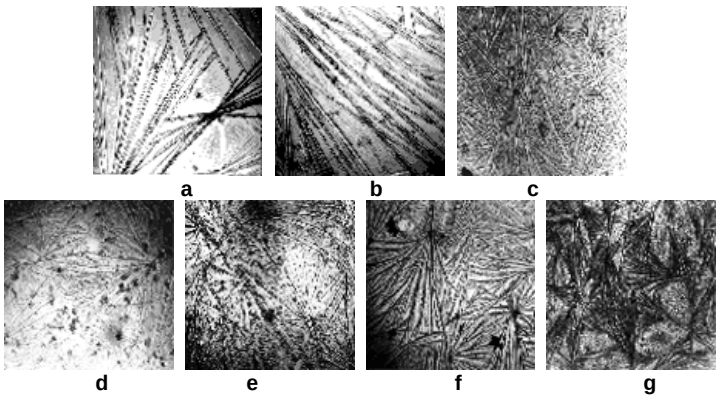

Figure 3. Crystallogram samples for the norm group (a-b) and for the pathology group (c-g)

To describe the gray level cooccurrence (GLC) matrix, we need the following definitions and symbols: D is the image field containing $M \times N$ pixels, $x_{m,n}$ is the gray value of pixel coordinates $(m,n) \in D$, G is the number of gray levels in the image. The indicator-function:

$$f_{i,j}(x_{m,n}, x_{m+k,n+l}) = \\ = \begin{cases} 1; & x_{m,n} = i \ , x_{m+k,n+l} = j \\ 0; & x_{m,n} \neq i \quad or \quad x_{m+k,n+l} \neq j \end{cases}; \qquad (9)$$

$$i, j = 0, 1, ..., \ G-1$$

shows, whether two neighboring pixels at the distance d have the determined levels.

Normalized values of the GLC matrix are defined as

$$P_{k,l}(i,j) = C_{k,l}(i,j) \Big/ \sum_i \sum_j C_{k,l}(i,j) \ , \qquad (10)$$

$$C_{k,l}(i,j) = \sum_{(m,n)\in D} \sum_{(m+k,n+l)\in D} f_{i,j}(x_{m,n}, x_{m+k,n+l}) \ , \qquad (11)$$

$$k,l = 0, \pm 1, \pm 2, \ ... \quad ,$$

The dimension of matrix $P_{k,l}$ is $G \times G$. The distinction between the opposite directions wasn't taken into account. Therefore, the symmetrical matrices $P^s_{k,l}$ were generated as follows: $P^s_{k,l} = \left(P_{k,l} + P_{-k,-l} \right) \Big/ 2$.

For the present purposes we chose to avoid the characterization of texture in a given direction. Each calculated matrix P^s_d is the average of four matrices calculated in the four directions (0°,45°,90° and 135°):

$$P^s_d = (P^s_{d,0} + P^s_{d,d} + P^s_{0,d} + P^s_{-d,d}) / 4 \ . \qquad (12)$$

A set of statistic features $F = \left(f^d_1, ..., f^d_6 \right)$ was calculated to summarize the GLC matrix. These features are textural features (Table 2). *Variance* describes the degree of image homogeneity. *Contrast* describes the degree of an image contrast. *Inertia* describes the presence of sharp edges. *Correlation* describes the degree of statistical dependence of pixels. *Shade* describes the degree of equiprobable appearance of dark and light areas in the image (the shade near the objects, etc.). *Entropy* is the measure of image disorder.

Table 2. The average nonnormalised values of each feature for major groups - norm and pathology

Feature	Norm	Pathology
Variance $f^d_1 = \sum_{i=0}^{G-1} \sum_{j=0}^{G-1} \left[P^s_d(i,j) \right]^2$	0,06	0,03
Contrast $f^d_2 = \sum_{i=0}^{G-1} \sum_{j=0}^{G-1} \lvert i-j \rvert P^s_d(i,j)$	0,08	0,14
Inertia $f^d_3 = \sum_{i=0}^{G-1} \sum_{j=0}^{G-1} (i-j)^2 P^s_d(i,j)$	2,1	4,2
Correlation $f^d_4 = \sum_{i=0}^{G-1} \sum_{j=0}^{G-1} (i-M_x)(j-M_x) P^s_d(i,j)$	25	40
Shade $f^d_5 = \sum_{i=0}^{G-1} \sum_{j=0}^{G-1} (i+j-M_x)^3 P^s_d(i,j)$	1,5	3,7
Entropy $f^d_6 = -\sum_{i=0}^{G-1} \sum_{j=0}^{G-1} \ln \left[P^s_d(i,j) \right] P^s_d(i,j)$	7,6	9,1

The K-nearest neighbors (KNN) method was applied to a series of images. The classifier was developed using randomly selected 50% of the data set, with the testing performed with the remaining 50% of data. With the KNN method, each pattern of the training set is stored as a prototype. The class of a new pattern is directly obtained from the computation of the distance between this pattern and each prototype in database. Among the KNN the majority class is affected to the unknown pattern.

Table 3. The classification results of the crystallograms samples

Class	a	b	c	d	e	f	g
Number of different samples	20	18	16	12	18	20	16
Number of samples in sets	200	180	160	120	180	200	160
Correctly classified	194	138	144	118	176	142	154
Rate of correct classification (%)	97.0	76.7	90	98	97	71	96

Group	Norm	Pathology
Correctly classified	334	810
Rate of correct classification (%)	87	98

As the number of samples in each class was relatively small, the classification was conducted ten times with various randomly selected testing and training sets. The classification rates presented in Table 3 correspond to the average results obtained in the experiments [5].

This results indicate the probability that the method of textural analysis will be used to determine the class of the crystallogram, and hence to determine the rate and type of the pathology, with a relatively small probability of false miss errors.

4. Conclusion

Methods of the direction field and statistical textural analysis have been used to construct a classifier that allows the lachrymal fluid crystallogram type to be determined. The fundamental possibility of using the technique for disease diagnostics has been proved. Some experiments yielded almost 95% accuracy.

It is possible to construct an expert system to diagnose the pathology type of biological liquid crystallograms. Additionally, the effectiveness and informativeness of the features were studied using the discriminant analysis method [6]. Since certain features are highly correlated with others the classification quality can be further improved. In future research, we propose to use a combination of textural and direction field analysis.

Acknowledgements: This work was financially supported by the U.S. Civilian Research and Development Foundation (CRDF) and the Ministry of Education of the Russian Federation international grant REC-SA-014-02 under Basic Research and Higher Education (BRHE) program.

References

1. Hozman, J., Bernas, M., Kubinek, R.:Biomedical Image Processing Applications. Biomedical Engineering & Biotechnology, Publishing House of the Czech Technical University (1994)
2. Ilyasova, N.Yu., Dvoryanova, T.P., Ustinov A.V., Khramov, A.G.: Computer-aided Analysis of the Tear-Crystal Image. Proceedings of 13-th biennal international conference Biosignal-96, Brno, (1996) 29-31
3. Soifer, V.A., Kotlyar, V.V., Khonina, S.N., Khramov, A.G.: The Method of the Directional Field in the Interpretation and Recognition of Images with Structure Redundancy. Pattern Recognition and Image Analysis, v.6, No.4, (1996) 710-724
4. Haralick, R.M., Shanmugam, K., Dinstein, I.: Textural features for image classification. IEEE Trans.Syst.Man Cybern. v.3, (1973), 610-621
5. Kupriyanov, A.V., Khramov, A.G. Ilyasova, N.Yu.: Statistical Features of Image Texture for Crystallogram Classification. Pattern Recognition and Image Analysis, vol. 11, No 1, (2001) 180-183
6. Kupriyanov, A.V., Khramov, A.G., Ilyasova, N.Yu.: Analysis of Features of Texture Images for Crystallogram Identification and Classification. Optical Memory & Neural Networks, vol.11, No.1, (2002) 19 - 28